BRILLOUIN OPTICAL TIME-DOMAIN ANALYZER ENGINEERED IMPLEMENTATION USING HIGH-ORDER POLYNOMIAL SPECTRAL FITTING

Alin JDERU[1], Dorel DOROBANTU[2], Marcelo A. SOTO[3], Marius ENACHESCU[2], Dominik ZIEGLER[1]

This work reports on the development and implementation of a first BOTDA (Brillouin optical time-domain analysis) sensing/detection platform in Bucharest, Romania. Our setup enables us to quantitatively determine temperature and strain in a few dozen kilometers long optical fibers. The engineered implementation uses a semiconductor optical amplifier to secure enhanced sensing performance, instead of using the more common electro-optical modulators employed to generate defined few nanosecond-long light pulses. In addition, we show that higher-order polynomial peak fitting can perform faster than Gaussian fitting and can provide a novel processing approach to extract the measuring information when the optical fiber exhibits more than a single Brillouin gain spectral peak. Our home-built BOTDA sensing platform exhibits LabVIEW based fully automated data acquisition and processing user interface. We demonstrate quantitative temperature measurements by using the engineered platform over a sensing/detection distance of 24 km with 2 m spatial resolution.

Keywords: Brillouin Optical Time-Domain Analysis, Fiber Optical Sensing, Temperature sensing

1. Introduction

In recent decades the optical fibers field has seen enormous growth. They cover a wide range of applications from shape or intrusion detection to structural health, power transmission lines and pipelines monitoring [1]. One of the key sensing methods is Brillouin optical time-domain analysis (BOTDA), which is a distributed sensing technique based on stimulated Brillouin scattering and allows measuring strain and temperature quantitatively over long distances [2]. Strain and temperature information are present in the peak frequency of the Brillouin gain spectrum (BGS), the so-called Brillouin frequency shift (BFS) of the sensing

[1] S.C. NanoPRO START MC. S.R.L, Bucharest, Romania,
[2] Faculty of Electronics, Telecommunications and Information Technology, University POLITEHNICA Bucharest, Romania, e-mail: marius.enachescu@cssnt-upb.ro
[3] Department of Electronic Engineering, Universidad Técnica Federico Santa María, 2390123 Valparaíso, Chile

fiber. In the BOTDA method, the BGS is monitoring the Brillouin scattering process that results from short optical pulses traveling along the fiber. In this work we present a new fully engineered implementation of this technique after a more detailed introduction to the method, we will describe the optoelectronic components of the sensing platform and we will discuss a few critical aspects which allowed us to obtain high-performance sensing, including i) clean generation of short optical pulses using semiconductor optical amplifiers ii) a novel method to fit the BGS with polynomial functions, and lastly iii) experimental demonstration of the proper functioning of the entire engineered setup by measuring variations in temperature with 2 m spatial resolution at a distance of over 20 km.

2. BOTDA sensing principle

Stimulated Brillouin scattering is a parametric process between a pump signal and a counter-propagating Stokes signal through an electrostriction-induced acoustic wave. As the interplay process takes place between these 2 signals (having a proper frequency difference), the acoustic wave results in a periodically modulated refractive index grating, which is scattering the pump wave by Bragg diffraction. Since the induced grating varies with time and position at fiber's acoustic velocity, the light that is scattered goes through a Doppler effect, inducing an optical frequency shift determined by acoustic frequency, corresponding to the so-called BFS [1], [2]. As per the total energy and momentum conservation law, the Brillouin scattered light is found to be back-scattered from the incident light wave.

Compared to Brillouin optical time-domain reflectometry (BOTDR), which is based on spontaneous Brillouin scattering (SpBS), Brillouin optical time-domain analysis (BOTDA) uses SBS to gain a higher sensitivity, thus leading to better sensing performance. In order to achieve SBS, BOTDA relies on a pump and probe method, in which a high-intensity pulse of a pump, while propagating, locally interacts with a faint continuous wave probe (CW). The Brillouin gain that the probe experiences on every location is analyzed by acquiring, for various frequency offsets, its time-domain amplitude, being around the BFS. The local Brillouin spectrum at certain frequency differences between the probe and the pump is retrieved and the local gain spectrum is, afterwards, rebuilt as a function of frequency [1], [2].

The main difficulty that this process brings is to scan the pump-probe frequency offset with steps of typically 1 MHz and a very high stability which must be much better than 1 MHz.

Given the high requirements to implement a reliable BOTDA system, one may conclude that the design and engineering tasks behind an engineered

implementation is quite challenging. While early demonstrations used two distinct lasers to induce SBS in the sensing fiber [3], the low reliability of the implementation to secure high spectral stability has led to the routinely implementation of using solutions based on a single laser source from which pump and probe signals are obtained, thus securing much higher steadiness of the pump and probe frequency offset [4]. The details of our implementation of this technique are discussed in the following.

3. Experimental Setup

Our engineered BOTDA sensor has been implemented as shown in Fig. 1, which shows the schematic of the optoelectronics (Fig. 1a), the conceptual CAD drawing used to optimize the assembly of all parts (Fig. 1b), and a photograph of the final assembled BOTDA sensor platform (Fig.1c).

One can see in the setup that the laser radiation (at 1550nm) is primarily divided with a 50:50 optical coupler. In the upper path, the wave of the probe is synthesized by an electro-optic modulator (EOM) actuated at the aimed pump-probe frequency offset by a microwave signal. A radio frequency generator which can be scanned over the Brillouin frequency shift range (~10.8GHz±100MHz) is used to drive the EOM. This EOM also requires to be biased by a proper direct-current voltage to run in a suppressed carrier diagram, thus enabling the use of the lower modulation sideband as a signal for probe. This experimental configuration is able to provide optimal stability as no laser frequency drift (resulting typically because of thermal changes) has an influence on the probe and pump frequency differences. To reduce the effects of SBS polarization, the polarization of the pump wave was switched prior of being launched in the fiber (FUT) via a polarization switch, so that by averaging two consecutive measurements at orthogonal polarizations we could efficiently cancel out the influence of the so-called SBS polarization fading. The optical power of both pump and probe signals is generally adjusted using Erbium-doped fiber amplifiers (EDFAs).

The generation of the pulse (counter-propagating with the probe signal in the fiber) is depicted in greater details in the following section of the paper. As, along the fiber, both pulse and probe counter-propagate, they interact with the glass core to induce an acoustic wave that drives the Brillouin optical gain over the probe signal at the Stokes wavelength. The amplified sideband of the probe is then isolated by a narrowband fiber Bragg grating (FBG) filter and a circulator. The filter fulfills the role of removing all the Rayleigh backscattering from the pump and the second probe sideband obtained during probe generation. A 100 MHz photodetector is employed to unravel the amplified signal of the probe and a fast data acquisition card and processing system plots and analyzes the BGS as a function of the fiber position.

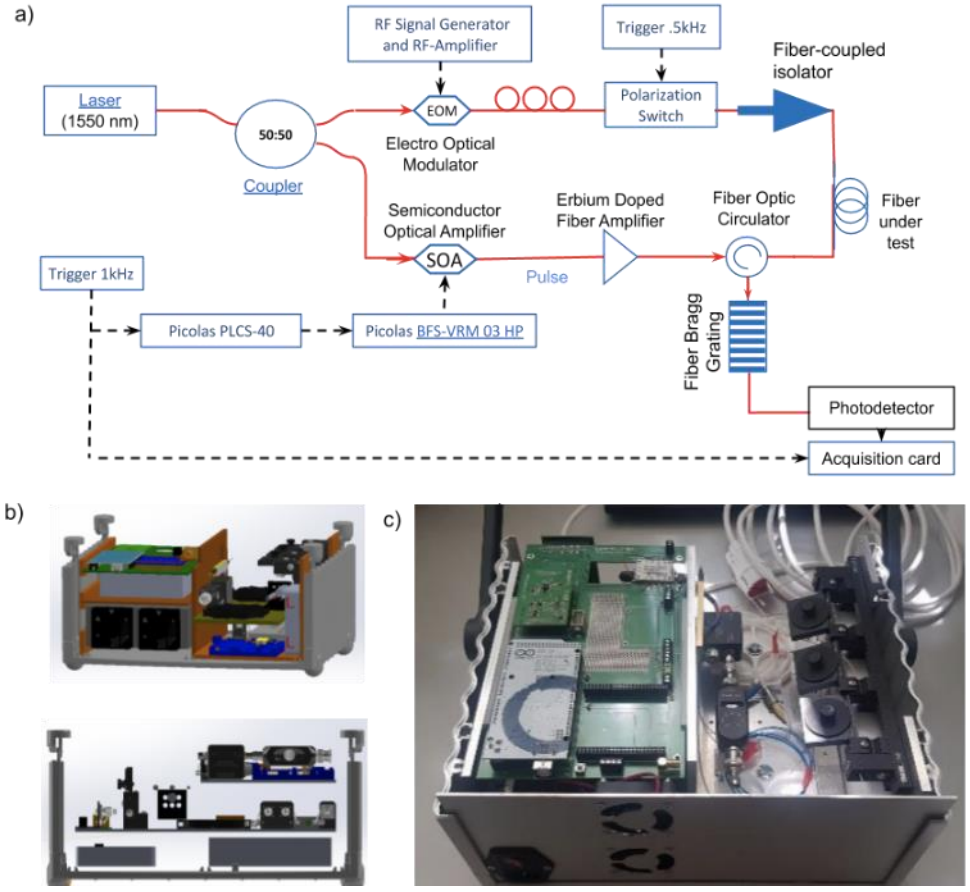

Fig. 1. a) Schematic of the optoelectronics of the implemented BOTDA system, b) CAD conceptions of the assembly of all optical components, c) photo of the realized BOTDA sensing platform with an open top lid.

Note that any BOTDA configuration imposes the ability to access both ends of the fiber because, within the sensing fiber, the CW probe and the pulse of the pump have to counter-propagate. For some applications this may be a limitation.

Furthermore, to achieve the maximum gain, given that the electrostriction stimulating the acoustic wave is induced by the interferences between the pump and signal, their polarization states should, preferably, be aligned.

When the polarizations of pump and probe are mutually orthogonal inside the optical fiber, that fiber position exhibits no Brillouin interaction, leading to so-called polarization fading. To avoid these unwanted fading, a straightforward solution is to use polarization-maintaining fibers as sensing fibers, however their high price makes them prohibitively expensive to reach sensing ranges of a few

kilometers or longer. When handling single-mode fibers, the polarization states of probe and pump randomly change throughout the fiber. The reason behind this phenomenon is the random fluctuations of the fiber birefringence caused by the core shape variations and the non-uniform stress acting on the core. This results in fiber locations having a fully efficient Brillouin interaction (at fiber positions when pump and probe have parallel polarizations) and locations with no SBS interaction at position with orthogonal polarizations. Interestingly, this polarization dependence of the Brillouin interaction can be used, favorably, to quantify optical fiber's local birefringence properties quickly and effectively.

4. Results

4.1 Pulse Generation

The generation of clean and only few nanosecond-long optical pulses with high-power and maximal suppression between two pulses, is a challenging task in the realization of any time-domain optical fiber sensing tool.

In our implementation, short electrical pulses are generated using an arbitrary waveform generator (AWG) (PLCS-40, PicoLAS, Germany) that drives the electro-optical intensity modulation. With the full range, analog real time modulation, this device can output arbitrary pulse shapes with a minimal pulse step duration of 1 ns. The voltage pulses are then converted into high-power current pulses using a high-speed laser driver (BFS-VRM 03 HP, Picolas Germany) highly suitable to drive a semiconductor optical amplifier (SOA - Thorlabs 1013SXS).

The use of an SOA for optical pulse shaping has significant advantages compared to other existing approaches. Compared to electro-optic modulators (EOMs), like conventional Mach Zehnder modulators, an SOA can provide a much higher pulse extinction ratio (normally > 50 dB), which means the quality of the optical pulse is highly improved. Indeed, the use of conventional EOMs (normally with an extinction ratio of 23 dB) results in optical pulses with a continuous wave pedestal, which does not contribute to the absence of light between optical pulses (during the off state of the pulses) in a BOTDA sensor. That CW light component highly impairs the performance of a BOTDA sensor by activating SBS along the entire fiber, providing a signal component with useless Brillouin information.

High-performance BOTDA sensing requires much higher extinction ratios, and even though there exist MZMs with 40 dB extinction ratio, an SOA provides even further improvements in the quality of the BOTDA measurements by reducing the interfering useless signal components in the measurements. Furthermore, compared to direct laser modulation, the optical pulses obtained by an SOA do not have the detrimental effect of chirps within the pulse width. The power of the short light pulses, before being released in one of the sensing fiber's

ends, is increased using a fiber amplifier doped with Erbium via a circulator. Fig. 2 shows the characterization of two distinct optical pulses generated using this technique.

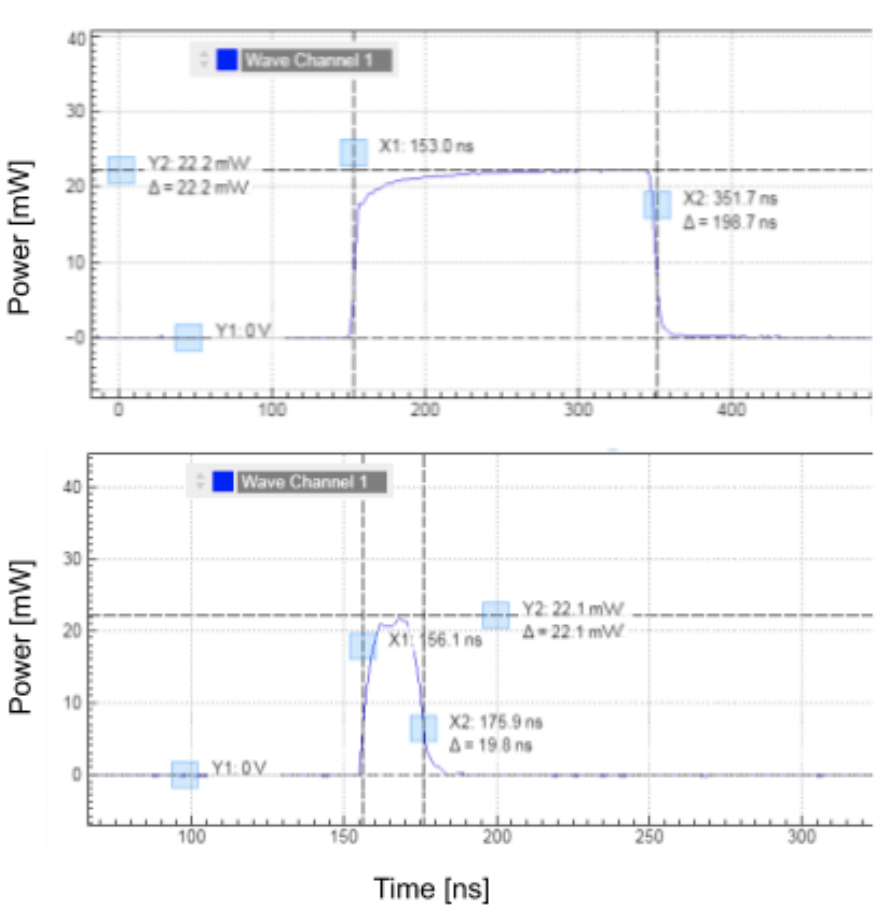

Fig. 2. The pulse length that can be implemented in the BOTDA setup is stepwise adjustable. In this case, a 22 nW optical pulses of 200 ns and 20 ns long are shown.

Table 1.

Characterization of the optical pulses obtained at the SOA output when driven by PicoLAS AWG

Set electrical pulse length (ns)	Active data points in the AWG	Measured optical pulse length (ns)	Measured pulse power (mW) uncorrected	Measured pulse power (mW) corrected
5	0	-[1]	-[1]	-[1]
8	1	2.4	8.7	18.4
10	2	5	14.7	22.1
20	7	15.9	19.0	22.1
50	19	47.6	21.0	22.1

100	39	98.5	21.1	22.1
200	79	197	22.2	22.2
320	128	320	22.2	22.2

[1] no optical output observed

To detect the optical pulses, we used a high-speed Indium Gallium Arsenide photodetector (DET08CFC, Thorlabs) and an acquisition board (DAC of UHFLI, Zurich Instruments) which allows observing the optical pulse lengths and peak powers.

Table 1, from above shows the resulting measured optical pulse lengths (normally shorter than the electrical pulses) and optical pulse powers for different settings of the electrical pulse lengths. We could generate and measure optical pulses down to 2.4 ns, however, for pulse lengths smaller than 20 ns we observed a decrease in the pulse power. Using the arbitrary waveform generator, we can easily correct for this drop effect by increasing the power which can be controlled digitally.

In our LabVIEW software this is done by creating a lookup table of the prerecorded values, we can set a gain to linearize the power pulses down below 10 ns. By correcting the power using a look-up table to drive more, we get a constant laser pulse power of 22 mW for pulse lengths down to below 5 ns. Having a short pulse length is important as it determines sensor's spatial resolution. This way, a pulse of 5 ns leads to a spatial resolution of 0.5 m. Defined by the pulse peak power and the power level ration in the off state (CW pedestal light), we could find an extinction ratio of about 50dB for the implemented system. This is substantially better than the 23dB that can be achieved typically with EOMs. The results in the next sections are obtained with an optimized optical pulse of 20 ns-long, securing distributed sensing with 2 m spatial resolution.

4.2 Polynomial Peak Fitting

A sequence of analyses is post-processed to identify, for each location of the fiber, BGS maximum amplitude's frequency which is, subsequently, enabling the extraction of the strain and local temperature [5], [6], [7], [8], [9]. Practically, this involves fitting the recorded spectral data which could be achieved by tuning, as example, the parameters of 2 curves, either Gaussian, Lorentzian or pseudo-Voigt, with a nonlinear least-squares regression. On the other hand, a fitting like this can be performed iteratively, thus possibly involving highly extensive times for processing, which cannot be used especially when rapid analyses are needed together with many data points along the full sensing fiber.

This work shows that much faster fitting can be achieved by using a higher-order polynomial fitting technique. The extraction of local temperature or strain information across the fiber, can be performed by post-processing the measured data to identify the BGS peak frequency at each location of the fiber [5], [6], [7], [8], [9]. Though modern methods to process the signal were proposed

recently, for local BFS retrieving fitting procedures, for instance quadratic, Voigt, Lorentzian or Gaussian curves are the most frequently used methods. The fitting techniques provide the ability to reliably and accurately extract the BFS under numerous scenarios.

Fig. 3 a) compares five different order polynomial fitting with orders ranging from 2nd to 10th as well as Gaussian fitting.

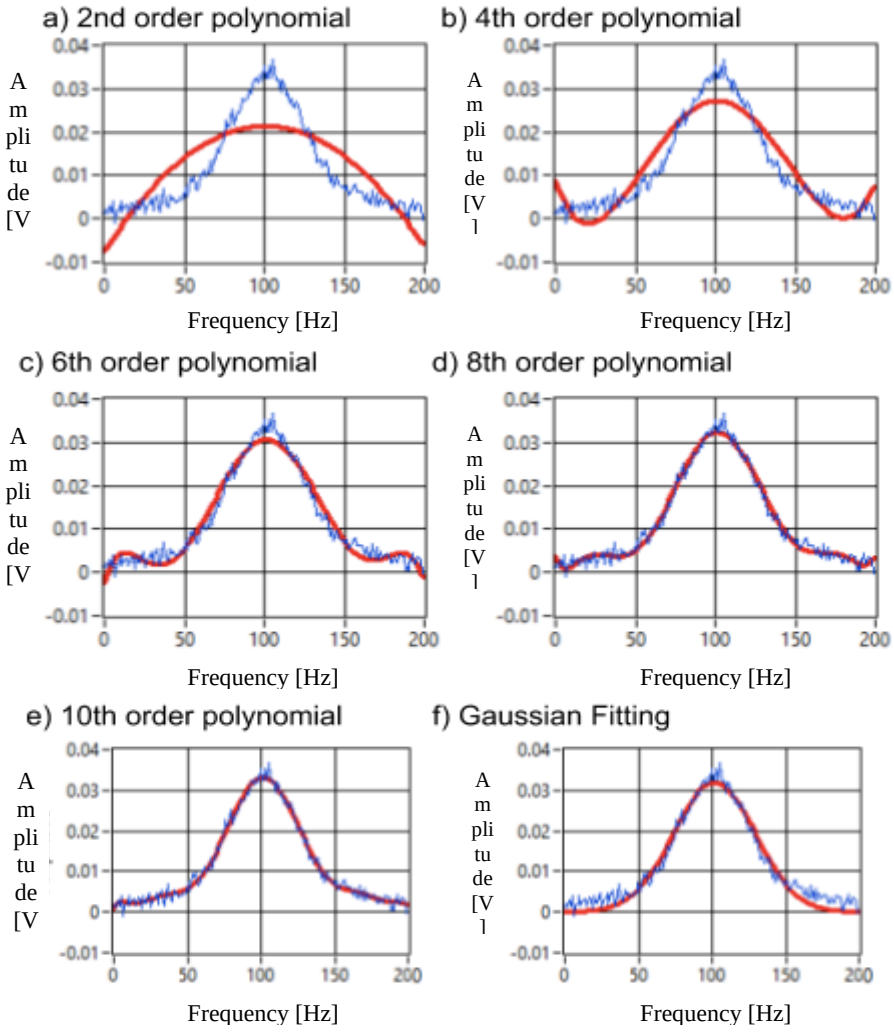

Fig 3. a)-e) Polynomial fitting with increasing order over 200 data points centered around the Brillouin gain peak. f) Gaussian fitting

We observed that the time for computation using polynomial fitting rises with the fitting order, linearly. Implemented in LabVIEW, the Gaussian fitting

took 24 minutes to fit all the 65000 data sets. However, even with a 10^{th} order fit it only took 35s to fit all the data sets [10].

This corresponds to a more than 40-fold improvement in computation speed and results in a peak location that matches the data obtained by Gaussian fitting very well. To save computation time, BOTDA implementations typically use low order polynomial fits, i.e. parabolic fits. As shown in Fig. 3 a), 2^{nd} order polynomial fits do not work to fit the entire BGS shape, and for this reason only a selected subset of the data can be used [8]. For instance, only the data points which are above half the peak amplitude can be taken into consideration in the fitting, along with an iterative procedure that avoids eventual bias in the BFS retrieval.

Fig. 3 a)-e) show higher-order polynomial fittings of even order. Clearly for a polynomial order of higher than 8^{th} or 10^{th}, the polynomial fittings match the entire spectral data very well, even better than the Gaussian fits shown in Fig. 3 f). An interesting aspect of polynomial fitting is that one could even obtain locations of multiple Brillouin frequency shifts. This would be useful for optical fibers which exhibit more than one acoustic resonance, were parabolic, Gaussian or Lorenztian fitting will fail in this case.

As shown in the next section, we can use the derivative of the polynomial function to find the peak location, this operation is significantly faster than Gaussian fitting. It is not uncommon to experimentally observe measurements with double Brillouin spectral peaks as shown in Fig. 4. Such phenomena could be generated by various reasons, as the fiber can for instance have multiple acoustic modes [11], or a poor extinction ratio revealed by the pulse of pump [12], or by the appearance of sharp/longitudinal transitions in temperature and strain [13], [14], [15].

The fitting methods used for single peak data have high probability in being unreliable to extract BFS in case of a sensing fiber with 2 Brillouin peaks, ultimately imposing the usage of more complex fitting algorithms. Fig. 4 shows a 2^{nd} and 6^{th} order polynomial regressions performed over the Brillouin spectral measurement of an optical fiber having two BGS peaks. Unsurprisingly, the maximum of the 2^{nd} order polynomial fit does not coincide with the measured peak values, i.e. it cannot be used for fitting a double peak. However, for the 6^{th} order polynomial both peak values can get much more accurately extracted by using the zeros of the derivative of the polynomial.

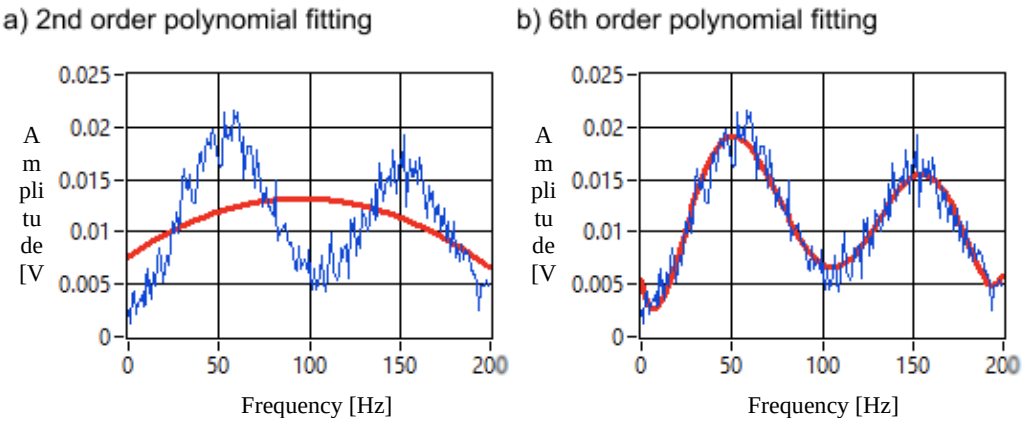

Fig. 4. a) 2nd order polynomial clearly cannot fit a double peak, b) a higher-order polynomial however, can adequately follow the BGS shape with a double peak (a 6th order polynomial fit). The frequency axis indicates steps of 1MHz.

4.3 Long-Distance Temperature Measurements

To fully test the entire setup, a sensing fiber range of ~24 km long is used. The first 21 km of sensing fiber corresponds to a standard unimodal fiber, which is maintained at room temperature during experiments. Then, a second spool of optical fiber (Corning SMF-28 (TM fiber CPC6)) with 2.5 km long is fully immersed in a water bath as shown in Fig. 5, where different temperatures are tested.

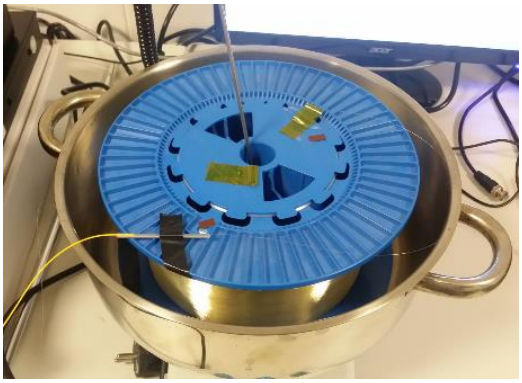

Fig. 5. Photo of the last 2.5 km of the sensing fiber (Corning SMF-28 (TM fiber CPC6)) as it is immersed in a water bath. Note that the first 21 km segment of the sensing fiber corresponds to a standard fiber spool that remains at room temperature during the experiment.

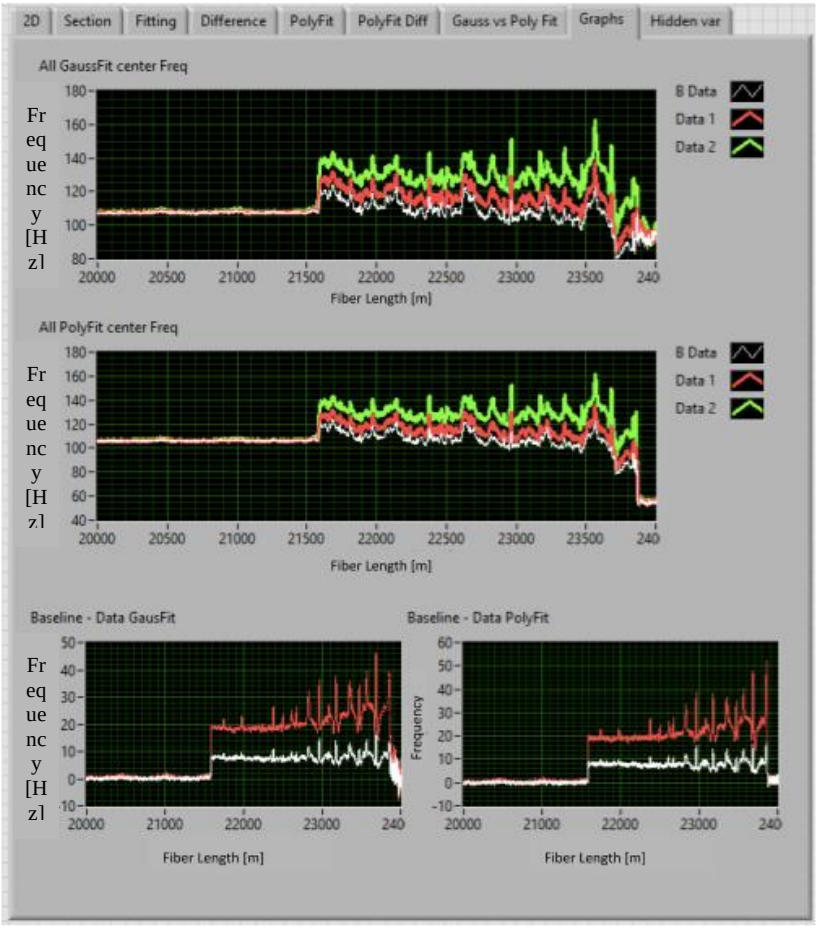

Fig. 6. Screenshot of the LabVIEW User interface that compares Gaussian Fitting and Polynomial Fitting for the determination of the frequency shifts along the optical fiber. The green, red, and white curves show the recordings for a temperature of 25ºC, 33ºC, and 45ºC respectively.

Fig. 6 shows part of the LabVIEW user interface which fully controls data acquisition and processing, including fitting and visualization. In particular, the screenshot compares Gaussian and Polynomial fitting for frequency shifts evaluation throughout the fiber. While the two first figures show the retrieved BFS profile in MHz with respect to the firstly scanned frequency of 10.7 GHz, the last two curves represent the frequency variation (in MHz) with respect to the reference trace obtained at 25ºC. The green, red, and white curves show the retrieved BFS profiles for a temperature of 25ºC, 34ºC, and 45ºC, respectively. We can observe that the proposed high-order polynomial fitting results in similar retrieved BFS profiles compared to a conventional Gaussian fitting. The frequency steps shown in the result match the expected values based on the

applied temperature steps. Note that the sharp periodic peaks along all the BFS traces can be attributed to periodic strain induced from wrapping the optical fiber onto the coil.

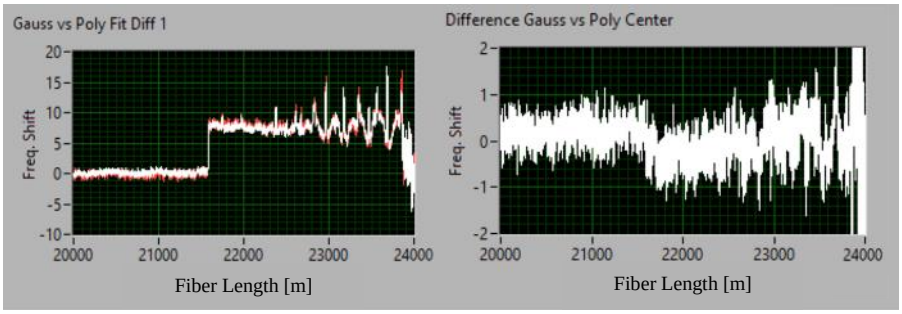

Fig. 7. Overlaid frequency shifts in MHz for polynomial and Gaussian Fitting (left), their difference (right) is throughout most of the fiber smaller than +/- 1MHz.

Fig. 7 compares the two fitting methods implemented, obtained when the dataset was recorded at 33ºC, and only the fitting algorithm was modified. The difference between the Gaussian fitting and the 10th order polynomial fitting method is smaller than +/- 1 MHz. This corresponds to a deviation in the observed temperature of roughly +/- 1ºC, however obtained in about 40-fold shorter processing times for the polynomial fitting case.

5. Conclusions

Here we reported the development of a long-range, high-performance fiber optical sensing platform based on the classical BOTDA method to monitor temperature (and strain) in optical fibers. We showed that an integrated sensing/detection platform, containing all optoelectronic components in a compact housing, has been designed and implemented successfully. In contrast to many commercially available implementations, we used an SOA instead of an EOM to achieve clean optical pulses with high extinction ratios. The used driver electronics allows to set the pulse length from a few nanoseconds to 320ns, thus covering a potential range of spatial resolutions from sub meter to 32 m.

The entire system is controlled from a LabVIEW user interface especially developed for controlling all optoelectronic components and allowing for data acquisition and advanced data analysis. The proposed higher-order polynomial fitting has shown to reach more than 40-fold improvement in computation time compared to a Gaussian fitting method.

To demonstrate the performance of our instrument, we demonstrated first temperature measurements over the entire length of a 24-kilometer-long fiber. The

measured and processed data show that we can quantitatively measure a temperature change that was applied close to 25 km sensing distance.

Funding:

This work was financed by the Romanian Ministry of Education and Research financing contract no. 34/01.09.2016, ID: P_37_788, MySMIS: 103364, project co-funded by the European Regional Development Fund through the Competitiveness Operational Program.

R E F E R E N C E S

[1]. *A. Motil, A. Bergman, and M. Tur*, "State of the art of Brillouin fiber-optic distributed sensing", Optics & Laser Technology, **78**(A), 81–103 (2016).

[2]. *M. A. Soto, Distributed Brillouin Sensing*, "Time-Domain Techniques" in Handbook of Optical Fibers, G.-D. Peng (ed.), Springer Nature Singapore Pte Ltd. (2018).

[3]. *T. Horiguchi, T. Kurashima, and M. Tateda,* "Technique to measure distributed strain in optical fibers," IEEE Photonics Technology Letters, vol. **2**, pp. 352-354, 1990.

[4]. *M. Nikles, L. Thévenaz, and P. A. Robert,* "Simple distributed fiber sensor based on Brillouin gain spectrum analysis," Optics letters, vol. **21**, pp. 758-760, 1996.

[5]. *M. A. Farahani, E. Castillo-Guerra, and B. G. Colpitts*, "Accurate estimation of Brillouin frequency shift in Brillouin optical time domain analysis sensors using cross correlation", Opt. Lett. **36**(21), 4275–4277 (2011).

[6]. *S. M. Haneef and K. Srijith, D. Venkitesh and B. Srinivasan*, "Accurate determination of Brillouin frequency based on cross recurrence plot analysis in Brillouin distributed fiber sensor," in 25th International Conference on Optical Fiber Sensors, 103239M (2017).

[7]. *S. M. Haneef, Z. Yang, L. Thévenaz, D. Venkitesh, and B. Srinivasan*, "Performance analysis of frequency shift estimation techniques in Brillouin distributed fiber sensors," Opt. Express 26, 14661-14677 (2018).

[8]. *M. A. Soto, and L. Thévenaz*, "Modeling and evaluating the performance of Brillouin distributed optical fiber sensors," Opt. Express 21, 31347-31366 (2013).

[9]. *Y. Zhang, D. Li, X. Fu, and W. Bi,* "An improved Levenberg–Marquardt algorithm for extracting the features of Brillouin scattering spectrum," Meas. Sci. Technol. 24(1), 015204 (2013).

[10] *Marcelo A. Soto, Jderu Alin, Dorel Dorobantu, Marius Enachescu, Dominik Ziegler*, "High-Order Polynomial Fitting Assistance for Fast Double-Peak Finding in Brillouin-Distributed Sensing," Sensors 21 (2020).

[11]. *X. Liu and X. Bao,* "Brillouin Spectrum in LEAF and Simultaneous Temperature and Strain Measurement," J. Lightwave Technol **30**(8), 1053-1059 (2012).

[12]. *H. Iribas, J. Mariñelarena, C. Feng, J. Urricelqui, T. Schneider, and A. Loayssa,* "Effects of pump pulse extinction ratio in Brillouin optical time-domain analysis sensors," Opt. Express 25, 27896-27912 (2017).

[13]. *A. W. Brown, M. D. DeMerchant, X. Bao, and T. W. Bremner,* "Spatial resolution enhancement of a Brillouin distributed sensor using a novel signal processing method," J. Lightwave Technol. **17**(7), 1179 (1999).

[14]. *S. Diakaridia, Y. Pan, P. Xu, D. Zhou, B. Wang, L. Teng, Z. Lu, D. Ba, and Y. Dong*, "Detecting cm-scale hotspot over 24-km-long single-mode fiber by using differential pulse pair BOTDA based on double-peak spectrum," Opt. Express **25**, 17727-17736 (2017).

[15]. *X. Sun, X. Hong, S. Wang, X. Gao, H. Guo, Y. Li, J. Qiu, and J. Wu*, "Frequency shift estimation technique near the hotspot in BOTDA sensor," Opt. Express **27**, 12899-12913 (2019).